Journal of Applied Electrochemistry (2007) 37:345–351
DOI 10.1007/s10800-006-9264-2


# Influence of bath composition and pH on the electrocodeposition of alumina nanoparticles and copper

ANDREAS BUND* and DENNY THIEMIG
*Institute of Physical Chemistry and Electrochemistry, Dresden University of Technology, D-01062, Dresden, Germany (*author for correspondence, tel.: +49-351-46334351, e-mail: andreas.bund@chemie.tu-dresden.de)*

Received 21 June 2006; accepted in revised form 15 October 2006

*Key words:* alumina, copper, dispersion coatings, electrocodeposition

**Abstract**

The electrocodeposition of alumina particles (primary particle size 13 nm) in a copper matrix was investigated. Three copper plating baths covering a wide pH range were used: an acidic copper sulphate, a neutral pyrophosphate, and an alkaline sorbitol based bath. The highest amount of incorporated particles (ca. 11 wt% alumina) was found for the pyrophosphate bath. From zeta potential measurements in diluted solutions we concluded that the particles are charged negatively in this electrolyte. A tentative electrostatic model is proposed to explain qualitatively the relation between the surface charge of the particles and the amount of incorporated particles. Furthermore, the microstructure, microhardness and electric conductivity of the layers were characterized.

## 1. Introduction

Composite coatings from nano-sized particles and metals are promising candidates for advanced surface finishing applications. The inclusion of hard particles such as silicon carbide and alumina in a metal matrix can yield advanced materials with high hardness and wear resistance. Usually particle concentrations between 1 and 10 volume percent have a beneficial effect. A well established system is Ni/SiC which is applied to increase the wear resistance of surfaces in combustion engines [1]. Another successful system is Ni/PTFE which combines the good mechanical and corrosion stability of Ni with the self-lubrication properties of PTFE [2–4].

There are a large number of useful metal/particle combinations and their possible applications. However, just putting the particles in a commercial plating bath and electroplating with the standard parameters usually does not work. In most cases coagulation and sedimentation of the particles occurs which makes successful codeposition impossible. Even if one succeeds in obtaining a more or less stable suspension the codeposition of the particles in the growing metal matrix might not work, at least not in considerable amounts. The reasons for this are not yet fully understood. It is generally accepted that the surface properties of the particles (charge, hydrophilic/hydrophobic), the characteristics of the metal deposition process (current density) and the hydrodynamic conditions in the cell are important parameters which govern the particle incorporation rate [5–7]. Several models have been proposed which describe the influence of some of these parameters [8–10]. However there is no complete understanding of the interaction of all the parameters. This paper focuses on the role of particle surface charges and the electrode in the $Cu/Al_2O_3$ system. There is controversy over the role of surface charge in the electrocodeposition process. Gugliemi stated ''both [electrophoresis and adsorption] can be supported by some arguments and contradicted by others'' [8]. Erler et al., reported that ''transport of particles by means of electrophoresis or their migration within the electrolyte [are] highly unlikely'' [11]. On the other hand Vidrich et al., argued that ''the particles need a positive net charge to be attracted via electrophoretic force by the cathode'' [12].

It is a challenging task to determine the surface charge of particles in a real plating bath. The usual procedures based on electrokinetic phenomena do not work well in media of high ionic strength. According to Newman the zeta potential is a property of the dielectric-solution interface and is due to the amount of specific adsorption at that interface [13]. It is roughly associated with the potential at the inner limit of the diffuse layer (shear plane in terms of zeta potential measurements), i.e. the outer Helmholtz plane. With increasing ionic strength the thickness of the diffuse double layer around the particle decreases and the potential at the shear plane becomes virtually the same as in the bulk solution. In other words no zeta potential can be measured under these conditions. Apart from this a variety of instrumental problems arise in electrolytes of high ionic strength such as short circuiting of the electric field

needed for the measurement. Therefore, in the present work we measured the zeta potential of the particles in dilute solutions of the components of the plating baths. Using this procedure it should be possible to estimate at least the sign of the particle surface charge under real plating conditions [11, 12].

The system $Cu/Al_2O_3$ was chosen; this is not widely applied on an industrial scale but has the potential for hard and wear-resistant coatings for electrical contacts. Three different copper electrolytes which cover almost the complete pH range were investigated.

## 2. Experimental

Pure copper and composite ($Cu/Al_2O_3$) coatings were electrochemically deposited from an acidic sulphate bath, a neutral pyrophosphate bath and an alkaline bath containing sorbitol [14]. These three electrolytes cover the pH range 1.7–12.5 (Table 1).

The alumina nanoparticles were commercially available (Aeroxide Alu C, Degussa) with an average diameter of 13 nm and a specific BET-surface of 100 $m^2\ g^{-1}$. The particles were kept in suspension using a magnetic stirrer. A double walled glass cell of volume 300 ml was used and the temperature was controlled with a Haake thermostate (model G D1, accuracy $\pm 1$ °C). The copper disk cathode with an active area of 0.08 $dm^2$, was vertically centred and surrounded by a cylindrical copper counter electrode of area 12 $dm^2$. The copper substrates were ground using 4000 grade silicon carbide paper, electrochemically degreased and activated with Uniclean 675 solution (Atotech Germany GmbH). The codeposition was carried out galvanostatically with a potentiostat/galvanostat model 273 (EG&G Princeton Applied Research) from electrolytes containing up to 10 g $l^{-1}$ $Al_2O_3$ powder with a current density between 1 and 10 A $dm^{-2}$. The thickness of the deposits ranged from 2 to 20 $\mu$m.

The zeta potential of the particles was determined with a Zetasizer 3 (Malvern Instruments, Herrenberg) using the principle of electrophoretic mobility. The zeta potential was measured in $10^{-3}$ M KCl with a concentration of 0.2 g $l^{-1}$ $Al_2O_3$ in the pH range 2–11. The pH was adjusted with HCl or KOH. The individual electrolyte components (Table 1) were added in concentrations of $10^{-3}$ M. Furthermore, dilute solutions of the electrolytes were prepared by mixing 0.02–0.1 ml of the corresponding electrolyte with 1 l of $10^{-3}$ M KCl. This dilution procedure is necessary to adjust the ionic strength of the solution to the requirements of the zeta potential measurement.

*Table 1.* Composition and working parameters of the three copper plating baths

| | Sulphate | Pyrophosphate | Sorbitol |
|---|---|---|---|
| pH | 1.7 | 7.4 | 12.5 |
| T/°C | 45 | 50 | 25 |
| Cu | 0.8 M $CuSO_4 \times 5H_2O$ | 0.6 M $Cu_2P_2O_7 \times 3H_2O$ | 0.6 M $CuSO_4 \times 5H_2O$ |
| other | 0.55 M $H_2SO_4$<br>3.26 mM HCl | 1.5 M $K_4P_2O_7$<br>0.05 M $C_6H_8O_7$<br>0.18 M $NH_3$ | 1.5 M $C_6H_{14}O_6$<br>3.0 M NaOH |

The potential of zero charge (pzc) of the copper-substrate was determined by electrochemical impedance spectroscopy (Zahner IM5d). The potential dependence of the double layer capacitance was measured in dilute electrolytes from $-400$ to $+100$ mV in steps of 50 mV (30 mHz–50 kHz). A standard calomel electrode (SCE KE10, Sensortechnik Meinsberg) was used as reference and a platinum mesh as counter electrode. For the extraction of the double layer capacitance a Randles equivalent circuit was assumed [15].

Scanning electron micrographs were recorded with a Zeiss DSM 982 (Oberkochen, Germany). The particle concentration in the layer was determined with energy dispersive X-ray analysis (EDX) on the surface of the coatings and over the cross section. The samples were embedded in epoxy resin and cut with a diamond saw. After mechanical grinding with 800–4000 grade silicon carbide paper and polishing with diamond suspensions down to 1 $\mu$m, the cross-sections were etched with 0.5 M nitric acid. The Vickers microhardness was measured in cross section with a FischerScope H100. Averaged values were calculated from 10 measurements per sample. The electrical resistance of the layers was determined with a four-point probe [16] using a lab-made sample holder and a RCL meter (Fluke, PM 6306). The layers for the resistance measurements were plated on a 0.9 $dm^2$ glass plate, which had been coated with 10 nm chromium (adhesion layer) and 50 nm copper by thermal evaporation.

## 3. Results and discussion

### 3.1. *Zeta potential of the particles*

In $10^{-3}$ M KCl the alumina particles had a positive zeta potential in the pH range from 2 to 9.5 with an isoelectric point (IEP) of 9.5 (Figure 1). Without complexing agents formation of copper(II)hydroxide in solutions containing 1 mM $Cu^{2+}$ starts at ca. pH 6.0. Therefore, measurements involving $CuSO_4$ cover only the pH range 2–6 in which the zeta potential of $Al_2O_3$ is slightly positive. In the presence of pyrophosphate bath the zeta potential is strongly shifted to negative values with an IEP of ca. 2.5. In the case of the alkaline sorbitol bath the pH dependence of the zeta potential is approximately the same as in $10^{-3}$ M KCl. The working pH of the electrolytes is 1.7 for the acidic sulphate, 7.4 for the pyrophosphate and 12.5 for the sorbitol bath (Table 1). From data shown in Figure 1 we can conclude that in the neutral and alkaline electrolytes the nanoparticles are charged negatively and in the acidic sulphate bath positively.

However, in the undiluted plating baths the structure of the electrical double layer (EDL) is different from

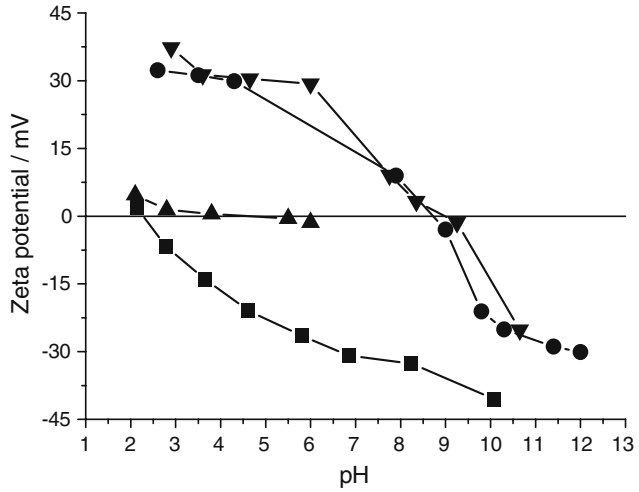


*Fig. 1.* Zeta potential of the 13 nm alumina nanoparticles (0.2 g $l^{-1}$) in different electrolytes as a function of pH (all concentrations are $10^{-3}$ M). (▼) KCl; (■) KCl + diluted pyrophosphate electrolyte; (▲) KCl + diluted sulphate electrolyte; (•) KCl + diluted sorbitol electrolyte.

that in the dilute electrolytes. Due to the high ionic strength the diffuse part of the EDL is very thin. As will be shown below in our cases the sign of the charge of the EDL is caused by specific adsorption of anions or cations on the particle surface [17].

To investigate how the individual components of the electrolytes affect the zeta potential we measured the zeta potential in the presence of selected components. Citric acid, potassium pyrophosphate and copper pyrophosphate shifted the zeta potential to negative values and the IEP to lower pH values (Figure 2). This is in accordance with the literature [18] where citric acid and potassium pyrophosphate are described as peptizing agents. The adsorption of these substances induces a negative surface charge, which leads to electrostatic stabilization of the dispersion. The addition of ammonia had no influence on the pH dependence of the zeta potential. Figure 3 shows that sulphate, either as sulfuric acid or as copper sulphate decreased the zeta potential in the pH range 2–6. The IEP in sulfuric acid is ca. 7.5. Thus it can be concluded that citrate, pyrophosphate and sulphate are adsorbed at the alumina surface and cause the shifts of the IEP.

### 3.2. *Impedance measurements – potential of zero charge*

From data presented above we can estimate the sign of the surface charge of the alumina particles under electroplating conditions. Now the question arises what will be the charge on the substrate under these conditions? As it is the cathode one would intuitively assume that the substrate is negatively charged. However the surface excess charge of an electrode depends on the position of the electrode potential with respect to the pzc of the electrode. Among other factors, the pzc depends on the electrolyte composition and surface treatment of the electrode. According to the Stern theory the double layer capacitance has a minimum at the pzc [19]. Using electrochemical impedance spectroscopy the potential dependence of the double layer capacitance of the copper substrates in the three dilute electrolytes was determined in the range from −0.3 to −0.05 V (Figure 4). From these data the following values of the pzc were estimated (all values vs. SCE): −0.3 V in the acidic copper sulphate electrolyte, −0.1 V in the neutral pyrophosphate electrolyte, and −0.15 V in the alkaline sorbitol electrolyte as shown in Figure 4. The pzc of the copper electrode in $10^{-3}$ M KCl was found to lie at −0.16 V vs. SCE (not shown) which is in good agreement with literature [20].

In the undiluted electrolytes the values of the double layer capacity will vary, but the general tendency of the pzc will be the same. Under electroplating conditions – i.e. current densities between −1 and −10 A $dm^{-2}$ – the potential of the working electrode was always cathodic

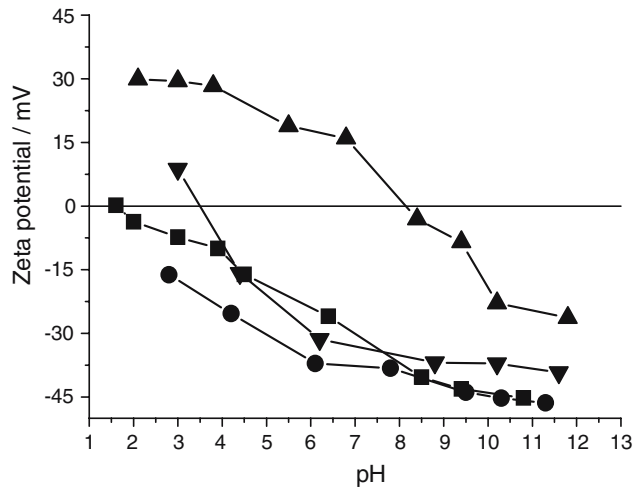


*Fig. 2.* Zeta potential of 0.2 g $l^{-1}$ $Al_2O_3$ nanoparticles in different electrolytes as a function of pH (all concentrations are $10^{-3}$ M). (▼) KCl + citric acid; (■) KCl + copper pyrophosphate; (▲) KCl + ammonia; (•) KCl + potassium pyrophosphate.

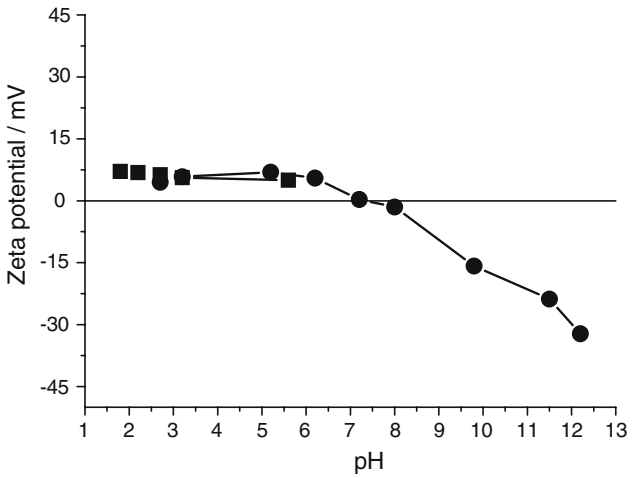


*Fig. 3.* Zeta potential of 0.2 g $l^{-1}$ $Al_2O_3$ nanoparticles in different electrolytes as a function of pH (all concentrations are $10^{-3}$ M). (■) KCl + copper sulphate; (•) KCl + sulfuric acid.

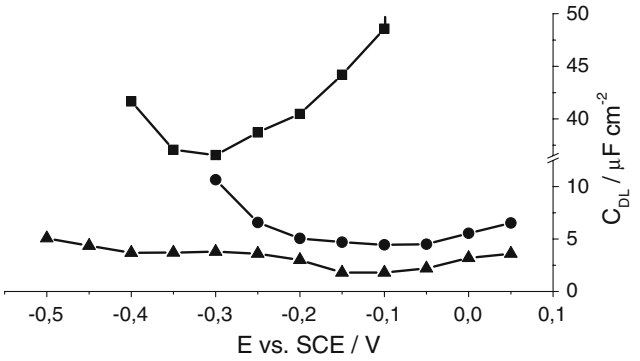


*Fig. 4*. Potential dependence of the double layer capacitance of the copper substrate in diluted electrolytes (0.1 ml l$^{-1}$). (■) copper sulphate electrolyte; (•) copper pyrophosphate electrolyte; (▲) sorbitol electrolyte.

from the above given pzc values. The metal electrode was negatively charged under the plating conditions.

### 3.3. *Particle content and microstructure of the layers*

The microstructure and the alumina concentration of the layers were investigated at the surface and in the bulk (cross section) using SEM and EDX. The alumina concentration of the layer increased with increasing concentration of $Al_2O_3$ in the electrolyte, in the case of the acidic (Figure 5(a)) and the alkaline sorbitol (Figure 5(c)) electrolyte. For the neutral pyrophosphate electrolyte the concentration went through a maximum or decreased slightly (Figure 5(b)) depending on the current density.

A general observation is the significant higher particle content of the layers deposited from neutral and alkaline electrolytes (Figure 5(b, c)) compared to the acidic electrolyte (Figure 5(a)). If we take into consideration that the particles are negatively charged in these electrolytes (Figure 1) this finding is difficult to rationalize. Why should a negatively charged particle be incorporated more easily than a positively charged one? Without detailed investigations of the interaction forces of the particles and the electrode, as suggested in the pioneering work of Dedeloudis and Fransaer [21], we can only speculate about the underlying mechanisms. The negative charge of the particles is due to a preferential adsorption of anions (citrate, pyrophosphate in our case). One possible explanation is that the negatively charged particles are attracted by the double layer of the substrate [22]. Under electroplating conditions this double layer should bear positive excess charges which interact with the negatively charged particles. The particles will also have a double layer around them, but this will be deformed. The particle is moving towards the electrode and the centre of its ionic shell lags a little bit behind. In the strong electric field of the double layer the hull of adsorbed anions is stripped off and the particle is incorporated into the growing metal matrix (Figure 6). This argument does not imply that electrocodeposition is completely governed by electrostatic forces. The proposed mechanism helps to rationalize the experimental results for the present system; negatively charged particles are incorporated in higher amounts than positively charged ones.

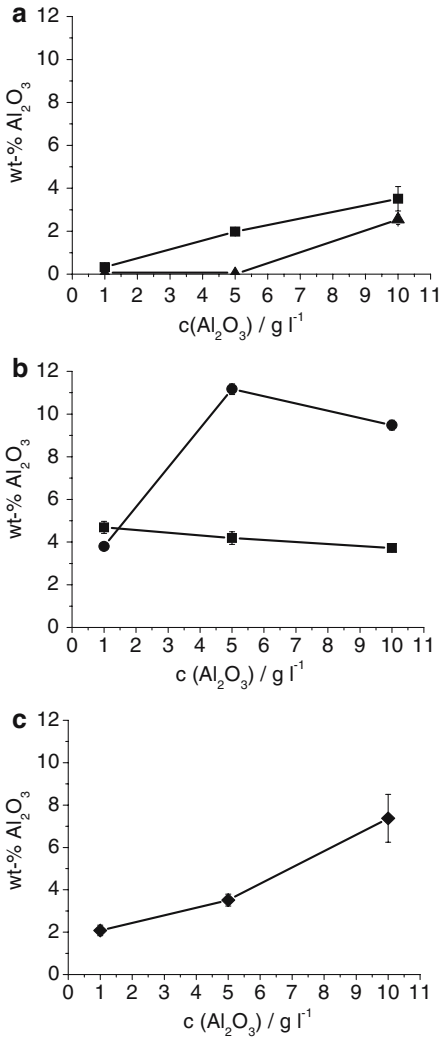


*Fig. 5*. Correlation between the $Al_2O_3$ content in the layer and the concentration of $Al_2O_3$ in the electrolyte for different current densities. (◆) 0.25 A dm$^{-2}$; (■) 1 A dm$^{-2}$; (▲) 5 A dm$^{-2}$; (•) 10 A dm$^{-2}$: (a) acidic sulphate electrolyte; (b) neutral pyrophosphate electrolyte; (c) alkaline sorbitol electrolyte.

High resolution SEM micrographs (not shown) indicated that at the sample surface the nanoparticles are mainly present as agglomerates with sizes of up to several hundred nanometres. Given the high ionic strength of the electrolytes this is the expected behaviour for alumina particles, the surface of which has not been treated specifically. In the case of composite coatings plated from the sorbitol bath embedded alumina particles could not be detected at the surface.

The layers deposited from the sorbitol bath had a powdery appearance and did not adhere well to the substrate. Therefore, they were not considered for the subsequent mechanical and electrical characterizations. The following discussion focuses on layers deposited from the copper sulphate and pyrophosphate bath.

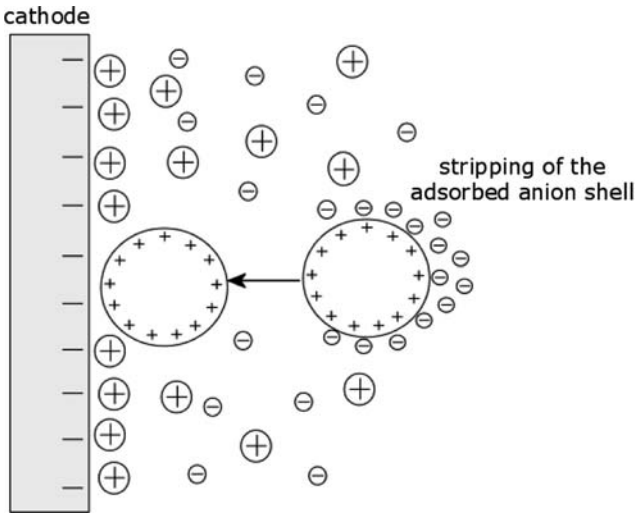


*Fig. 6*. Schematic representation of the charge distribution during electrocodepositon of the nanoparticles.

Figure 7 shows cross sectional SEM micrographs of pure copper layers formed from the sulphate bath (Figure 7(a)) and the pyrophosphate bath (Figure 7(b)). The coatings from the sulphate bath showed a columnar structure with relatively large grains. The films plated from the pyrophosphate bath are finer grained with a granular structure. From that we can already anticipate that the pyrophosphate layers should reveal a higher hardness. A general observation was that with increasing current density and content of alumina particles a refinement of the grains occurred, which is in agreement with results of Gan et al. [23].

In the case of the acidic sulphate bath the particle incorporation changed the microstructure from columnar to granular (Figure 8(a)). In the case of the pyrophosphate bath the microstructure remained granular (Figure 8(b)) but with a considerable refinement of the grains; the grain size was some hundred nm (micrographs not shown).

### 3.4. *Vickers microhardness of the copper coatings*

The Vickers microhardness of the copper layers varied between 70 and 270 HV. The literature values of coatings from the sulphate bath are 50–105 HV [24] and from the pyrophosphate bath 150–250 HV [25] depending on the electrolyte composition and the plating parameters. In accordance with the literature [26] the pure copper films plated from the sulphate bath were relatively soft (Figure 9(a)) whereas the films plated from the alkaline pyrophosphate bath showed a higher microhardness (Figure 9(b)).

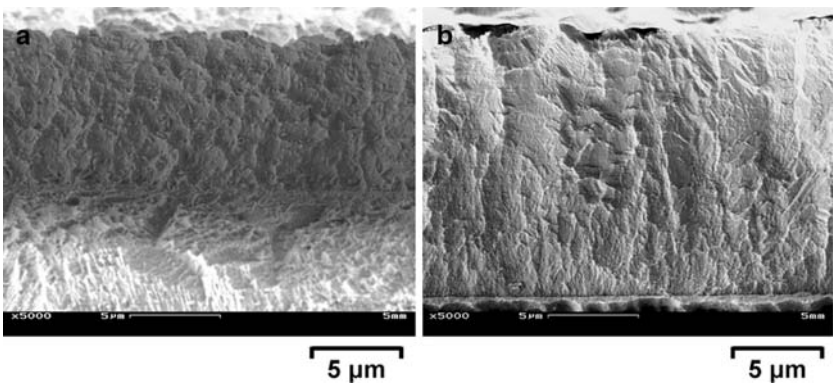


*Fig. 7*. Cross sectional scanning electron micrographs of pure copper films plated at 5 A $dm^{-2}$ from (a) acidic sulphate bath; (b) neutral pyrophosphate bath.

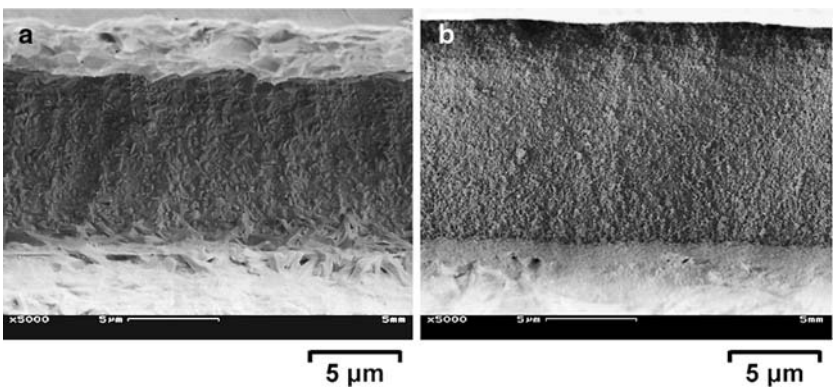


*Fig. 8*. Cross sectional scanning electron micrographs of composite coatings. (a) acidic copper sulphate, 5 A $dm^{-2}$, 5 g $l^{-1}$ $Al_2O_3$. (b) neutral copper pyrophosphate, 5 A $dm^{-2}$, 5 g $l^{-1}$ $Al_2O_3$.

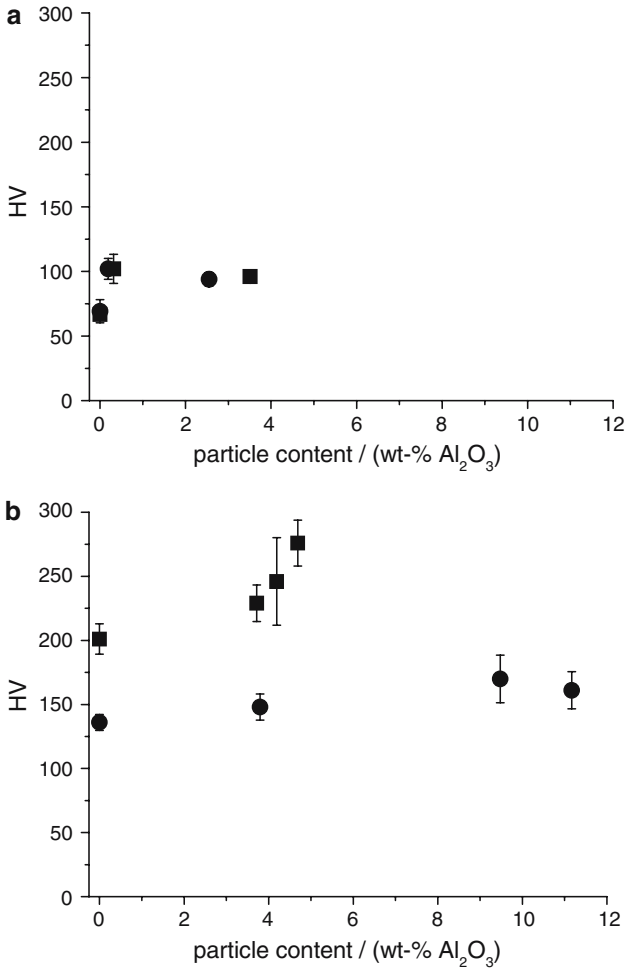


*Fig. 9.* Correlation between the $Al_2O_3$ content in the layer and the Vickers microhardness. (a) acidic sulphate electrolyte (■) 5 A $dm^{-2}$; (•) 10 A $dm^{-2}$. (b) neutral pyrophosphate electrolyte (■) 1 A $dm^{-2}$; (•) 5 A $dm^{-2}$.

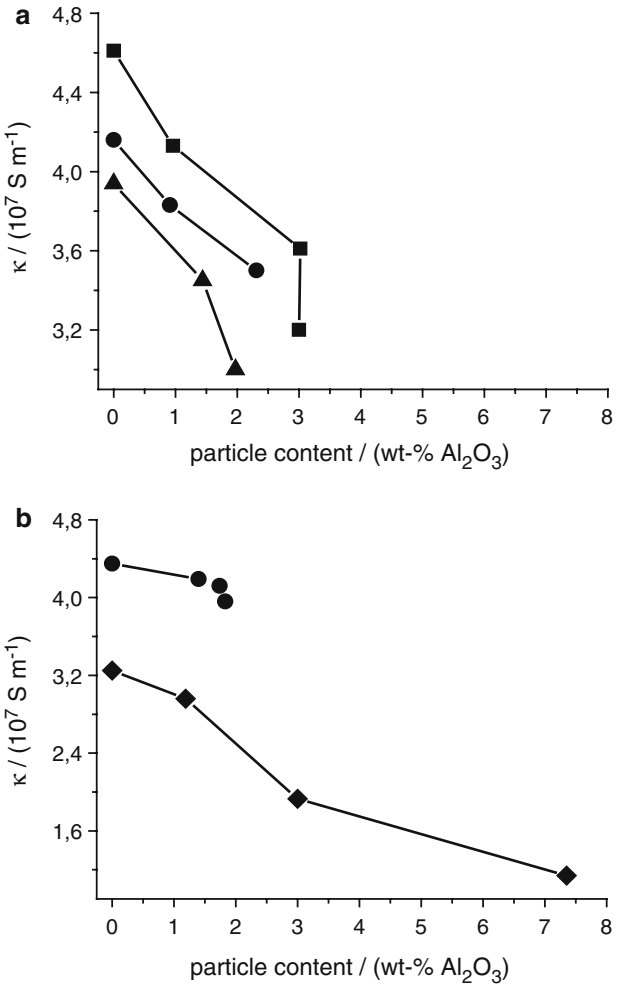


*Fig. 10.* Correlation between the $Al_2O_3$ content in the layer and the electrical conductivity. (a) acidic sulphate electrolyte (■) 3 A $dm^{-2}$; (•) 5 A $dm^{-2}$; (▲) 10 A $dm^{-2}$. (b) neutral pyrophosphate electrolyte (◆) 1 A $dm^{-2}$; (•) 5 A $dm^{-2}$.

The microhardness of the composite coatings was only slightly affected by the inclusion of particles (Figure 9). The effect of current density was more pronounced. Normally an increase in hardness is expected with increasing current density because of the decrease in grain size of the deposit. Interestingly, in the case of the pyrophosphate bath the hardness of the deposits decreased with increasing current density. This finding can be explained by the inclusion of phosphorus in the deposit [27, 28]. With decreasing current density the amount of incorporated phosphorus increases which renders the layer harder [28].

The coatings plated at lower current densities contained more $Al_2O_3$ and showed a higher microhardness (Figure 9). However, care must be taken when interpreting this increase in hardness as a direct consequence of the particle inclusion (such as "alumina is harder than copper, thus a mixture of both must be harder than copper"). It must be borne in mind that, as a consequence of particle inclusion, the microstructure becomes more granular and finer grained. Therefore, at least part of the hardness increase is due to changes in microstructure.

### 3.5. *Electric conductivity of the layers*

The electric conductivity of a metal layer should be directly related to its non-conducting particle content. Because one possible application of $Cu/Al_2O_3$ lies in the field of electrical contacts the dependence of the electrical conductivity was studied as a function of the amount of incorporated particles. Furthermore, electrical measurements might be a fast method to estimate the particle content of a composite coating.

The electric conductivity of the pure copper films was in the range of $3–5 \times 10^7\ \Omega^{-1}\ m^{-1}$ which agrees with literature [24, 29]. As expected, the electrical conductivity of the layers decreased with increasing particle concentration (Figure 10). Nevertheless, the conductivity is still sufficiently high for electric applications. Furthermore, due to the clear correlation between the electrical conductivity and the particle content an estimation of the latter from the former seems to be possible for a given deposition current. The electrical conductivity of an electroplated metal layer strongly depends on a variety of parameters, such as grain size, composition, and temperature [30]. Hence, the estima-

tion of the particle content of electroplated composite coatings is only possible if the operating conditions and their effect on the electrical conductivity are known.

In the case of the acidic electrolyte the conductivity of the layer decreases with increasing current density [27]. In contrast, the coatings plated from the neutral pyrophosphate electrolyte have higher conductivities if plated at higher current densities (Figure 10(b)). This finding can be explained in terms of changes in the microstructure of the layers as a function of plating current. It can be shown that an increased current density is related to a refinement in grain structure [27]. Plating at lower current densities also favours the codeposition of particles and phosphorus. As a result the electrical conductivity decreases [30].

## 4. Summary

It has been shown that the surface charge of particles is an important parameter for an electrocodeposition process. An interesting result was that negatively charged particles are better incorporated than positively charged particles. This finding, which is counterintuitive at first glance, has been explained in terms of an electrostatic model which takes into consideration the presence of ionic shells. The microhardness and electric conductivity of the layers have been characterized. The former is mainly governed by the microstructure of the layer whereas the latter clearly depends on the particle content.

## References


1. J.P. Celis and J. Fransaer, *Galvanotechnik* **88** (1997) 2229.
2. P. Bercot, E. Pea-Munoz and J. Pagetti, *Surf. Coat. Tech.* **157** (2002) 282.
3. S. Rossi, F. Chini, G. Straffelini, P.L. Bonora, R. Meschini and A. Stampali, *Surf. Coat. Tech.* **173** (2003) 235.
4. M.-D. Ger, K.-H. Hou and B.-J. Hwang, *Mat. Chem. Phys.* **87** (2004) 102.
5. J.B. Talbot, *Plat. Surf. Finish.* **91** (2004) 60.
6. V. Bouet, J. Fransaer, F. Huet, G. Maurin and J.P. Celis, *J. Electrochem. Soc.* **145** (1998) 436.
7. A. Hovestad and L.J.J. Janssen, *J. Appl. Electrochem.* **25** (1995) 519.
8. N. Guglielmi, *J. Electrochem. Soc.* **119** (1972) 1009.
9. J.P. Celis, J.R. Roos and C. Buelens, *J. Electrochem. Soc.* **134** (1987) 1402.
10. J. Fransaer, J.P. Celis and J.R. Roos, *J. Electrochem. Soc.* **139** (1992) 413.
11. F. Erler, C. Jakob, H. Romanus, L. Spiess, B. Wielage, T. Lampke and S. Steinhäuser, *Electrochim. Acta* **48** (2003) 3063.
12. G. Vidrich, J.-F. Castagnet and H. Ferkel, *J. Electrochem. Soc.* **152** (2005) C294.
13. J. Newman and K.E. Thomas-Alyea, *Electrochemical Systems*, 3rd edn, (Wiley Interscience, New Jersey, 2004).
14. L.L. Barbosa, M.R.H. de Almeida, R.M. Carlos, M. Yonashiro, G.M. Oliveira and I.A. Carlos, *Surf. Coat. Tech.* **192** (2005) 145.
15. A.J. Bard, M. Stratmann and P.R. Unwin, *Encyclopedia of Electrochemistry* Vol. 3 (Wiley VCH, Weinheim, 2003).
16. L.J. van der Pauw, *Philips Tech. Rundsch.* **59** (1958) 230.
17. Y. Zhang, Y. Fan, X. Yang, Z. Chen and J. Zhang, *Plat. Surf. Finish.* **91** (2004) 39.
18. R.H. Mueller, *Zetapotential und Partikelladung in der Laborpraxis* (Wissenschaftliche Verlagsgesellschaft mbH, Stuttgart, 1996).
19. A.J. Bard and L.R. Faulkner, *Electrochemical Methods. Fundamentals and Applications*, 2nd edn, (John Wiley and Sons, New York, 2001).
20. R. Landsberg and H. Bartelt, *Elektrochemische Reaktionen und Prozesse* (Deutscher Verlag der Wissenschaft, Berlin, 1977).
21. C. Dedeloudis and J. Fransaer, *Langmuir* **20** (2004) 11030.
22. F. Wuensche, A. Bund and W. Plieth, *J. Solid State Electrochem.* **8** (2004) 209.
23. Y. Gan, D. Lee, X. Chen and J.W. Kysar, *J. Eng. Mat. Tech.* **127** (2005) 451.
24. V.A. Lamb, C.E. Johnson and D.R. Valentine, *J. Electrochem. Soc.* **117** (1970) 291C.
25. N. Kanani, *Kupferschichten – Abscheidung, Eigenschaften und Anwendung* (Leuze Verlag, Bad Saulgau, 2000).
26. V.A. Lamb, C.E. Johnson and D.R. Valentine, *J. Electrochem. Soc.* **117** (1970) 381C.
27. M. Schlesinger and M. Paunovic, *Modern Electroplating*, 4th edn, (John Wiley and Sons, New York, 2000).
28. R.Y. Bek and G.N. Sorkin, *Izv. Sib. Otd. Akad. Nauk SSR, Ser. Khim. Nauk* **5** (1970) 142 (English translation available).
29. V.A. Lamb, C.E. Johnson and D.R. Valentine, *J. Electrochem. Soc.* **117** (1970) 341C.
30. G. Gottstein, *Physical Foundations of Materials Science* (Springer, Berlin, Heidelberg, 2004).